

Searching for supersymmetry in rare B decays

JoAnne L. Hewett, James D. Wells

*Stanford Linear Accelerator Center
Stanford University, Stanford, CA 94309[†]*

Abstract

We quantify the ability of B -Factories to observe supersymmetric contributions to the rare decays $B \rightarrow X_s \gamma$ and $B \rightarrow X_s l^+ l^-$. A global fit to the Wilson coefficients which contribute to these decays is performed from Monte Carlo generated data on $B(B \rightarrow X_s \gamma)$ and the kinematic distributions associated with the final state lepton pair in $B \rightarrow X_s l^+ l^-$. This fit is then compared to supersymmetric predictions. Evaluation of the Wilson coefficients is carried out with several different patterns of the superpartner spectrum. We find that B -Factories will be able to probe regions of the SUSY parameter space not accessible to LEP II, the Tevatron, and perhaps the LHC. We also employ the recent NLO calculation of the matrix elements for $B \rightarrow X_s \gamma$ and find the bound $m_{H^\pm} > 300$ GeV in two-Higgs-doublet models using present data.

[†]Work supported by the Department of Energy under contract DE-AC03-76SF00515.

1 Introduction

Softly broken supersymmetry (SUSY) is a decoupling theory, thus making it a challenge to search for its effects through indirect methods. When competing with standard model tree-level processes, the relative shift in an electroweak observable with respect to the standard model (SM) value should not be expected to exceed much more than $(\alpha_2/2\pi)M_W^2/\tilde{m}^2$. In the post-LEP II and Tevatron era, if supersymmetry has not been directly observed, then $\tilde{m} \gtrsim M_W$, and so the relative shift expected in standard model observables from virtual supersymmetry is $\lesssim 0.5\%$. Although the 1σ bounds on $\sin^2\theta_W$ are approaching this level from the analysis of SLC/LEP data, a more statistically significant result would be difficult to obtain given the current data sets available.

Another approach to indirect searches of supersymmetry is to measure observables where supersymmetry and the standard model arise at the same order in perturbation theory. In this case, the SUSY contributions do not suffer an extra $\alpha/4\pi$ reduction compared to the standard model amplitudes. The relative ratio between the lowest order standard model amplitudes and supersymmetric partner amplitudes could then be $\mathcal{O}(1)$ if $\tilde{m} \simeq M_W$. Rare B -decay measurements provide an opportunity for discovering indirect effects of supersymmetry by this second approach.

Two problems in the past have marred the attempts to use rare B decays as a good probe for physics beyond the standard model. The first is limited statistics, or rather the number of B mesons available in data sets which can be used to study and obtain good precision on low branching fraction modes. The B factories presently under construction, which will collect some 10^{7-8} B mesons per year, will alleviate this issue. The second difficulty is theoretical. Since all the processes occur near 5 GeV the uncertainties in the strong interactions can hide even $\mathcal{O}(1)$ effects in the electroweak contributions. However, this problem diminishes significantly [1, 2, 3] with a complete program of next-to-leading order (NLO) computations of the QCD corrections to rare B decays. For the processes we will consider here, $B \rightarrow X_s\gamma$ and $B \rightarrow X_s\ell^+\ell^-$, these higher order calculations have essentially been completed recently [4, 3, 5]. The inclusive decay $B \rightarrow X_s\gamma$ has been observed by CLEO [6] with a branching fraction of $(2.32 \pm 0.57 \pm 0.35) \times 10^{-4}$ and 95% C.L. bounds of $1 \times 10^{-4} < B(B \rightarrow X_s\gamma) < 4.2 \times 10^{-4}$. Meanwhile, experiments at e^+e^- and hadron colliders are closing in on the observation[7] of the exclusive modes $B \rightarrow K^{(*)}\ell^+\ell^-$ with $\ell = e$ and μ , respectively. Once this decay is observed, the utilization of the kinematic distributions of the $\ell^+\ell^-$ pair, such as the lepton pair invariant mass distribution and forward backward asymmetry [8, 9], and the tau polarization asymmetry [10] in $B \rightarrow X_s\tau^+\tau^-$, together with $B(B \rightarrow X_s\gamma)$ will provide a stringent test of the SM.

The outline of this paper is as follows. In section 2 we calculate the ability of future B -factories

to experimentally determine the magnitude and sign of the relevant Wilson coefficients in the rare B decay interaction Hamiltonian using a global fit procedure. We find that the sensitivity for new physics will be substantially increased beyond what is currently possible. In section 3 we apply these results to supersymmetry and estimate the sensitivity to high supersymmetric mass scales. We also reexamine the constraints on the H^\pm sector from $B \rightarrow X_s \gamma$, in light of the recent NLO computations. And in the final section we discuss our conclusions.

2 Determination of the Wilson coefficients

The effective field theory for the decays $B \rightarrow X_s \gamma$ and $B \rightarrow X_s \ell^+ \ell^-$, which incorporates the QCD corrections, is governed by the Hamiltonian

$$\mathcal{H}_{eff} = \frac{-4G_F}{\sqrt{2}} V_{tb} V_{ts}^* \sum_{i=1}^{10} C_i(\mu) \mathcal{O}_i(\mu), \quad (1)$$

where the \mathcal{O}_i are a complete set of renormalized operators of dimension six or less which mediate $b \rightarrow s$ transitions. These operators are catalogued in, *e.g.*, Ref. [11]. The C_i represent the corresponding Wilson coefficients which are evaluated perturbatively at the electroweak scale where the matching conditions are imposed and then evolved down to the renormalization scale $\mu \approx m_b$. We note that the magnetic and chromomagnetic dipole operators, $\mathcal{O}_{7,8}$, contain explicit mass factors which must also be renormalized.

For $B \rightarrow X_s \ell^+ \ell^-$ this formalism leads to the physical decay amplitude (neglecting the strange quark mass)

$$\begin{aligned} \mathcal{M}(B \rightarrow X_s \ell^+ \ell^-) = & \frac{\sqrt{2} G_F \alpha}{\pi} V_{tb} V_{ts}^* \left[C_9^{eff} \bar{s}_L \gamma_\mu b_L \bar{\ell} \gamma^\mu \ell + C_{10} \bar{s}_L \gamma_\mu b_L \bar{\ell} \gamma^\mu \gamma_5 \ell \right. \\ & \left. - 2C_7^{eff} m_b \bar{s}_L i \sigma_{\mu\nu} \frac{q^\nu}{q^2} b_R \bar{\ell} \gamma^\mu \ell \right], \quad (2) \end{aligned}$$

where q^2 represents the momentum transferred to the lepton pair. The expressions for $C_i(M_W)$ are given by the Inami-Lim functions[12]. A NLO analysis for this decay has recently been performed[4], where it is stressed that a scheme independent result can only be obtained by including the leading and next-to-leading logarithmic corrections to $C_9(\mu)$ while retaining only the leading logarithms in the remaining Wilson coefficients. The residual leading μ dependence in $C_9(\mu)$ is cancelled by that contained in the matrix element of \mathcal{O}_9 . The combination yields an effective value of C_9 given by,

$$C_9^{eff}(\hat{s}) = C_9(\mu) \eta(\hat{s}) + Y(\hat{s}), \quad (3)$$

with $Y(\hat{s})$ being the one-loop matrix element of \mathcal{O}_9 , $\eta(\hat{s})$ represents the single gluon corrections to this matrix element, and $\hat{s} \equiv q^2/m_b^2$ is the scaled momentum transferred to the lepton pair. The effective value for $C_7^{eff}(\mu)$ refers to the leading order scheme independent result obtained by Buras *et al.* [2]. The corresponding formulae for $C_i(\mu)$, $Y(\hat{s})$ and $\eta(\hat{s})$ are collected in Refs. [4, 11]. The operator \mathcal{O}_{10} does not renormalize and hence its corresponding coefficient does not depend on the value of μ (except for the μ dependence associated with the definition of the top-quark mass). The numerical estimates (in the naive dimensional regularization (NDR) scheme) for these coefficients are then (taking $m_b^{pole} = 4.87$ GeV, $m_t^{phys} = 175$ GeV, and $\alpha_s(M_Z) = 0.118$)

$$\begin{aligned} C_7^{eff}(\mu = m_b \begin{smallmatrix} -m_b/2 \\ +m_b \end{smallmatrix}) &= -0.312_{+0.034}^{-0.059}, \\ C_9(\mu = m_b \begin{smallmatrix} -m_b/2 \\ +m_b \end{smallmatrix}) &= 4.21_{-0.40}^{+0.31}, \end{aligned} \quad (4)$$

and

$$C_{10}(\mu) = -4.55. \quad (5)$$

The reduced scale dependence of the NLO versus the LO corrected coefficients is reflected in the deviations $\Delta C_9(\mu) \lesssim \pm 10\%$ and $\Delta C_7^{eff}(\mu) \approx \pm 20\%$ as μ is varied in the range $m_b/2 \leq \mu \leq 2m_b$. We find that the coefficients are much less sensitive to the values of the remaining input parameters, with $\Delta C_9(m_b), \Delta C_7^{eff}(m_b) \lesssim 3\%$, varying $\alpha_s(M_Z) = 0.118 \pm 0.003$ [13, 14], and $m_t^{phys} = 175 \pm 6$ GeV [15] corresponding to $m_t(m_t) = 166 \pm 6$ GeV. The resulting inclusive branching fractions (which are computed by scaling the width for $B \rightarrow X_s \ell^+ \ell^-$ to that for B semi-leptonic decay) are found to be $(6.25_{-0.93}^{+1.04}) \times 10^{-6}$, $(5.73_{-0.78}^{+0.75}) \times 10^{-6}$, and $(3.24_{-0.54}^{+0.44}) \times 10^{-7}$ for $\ell = e, \mu$, and τ , respectively, taking into account the above input parameter ranges, as well as $B_{sl} \equiv B(B \rightarrow X \ell \nu) = (10.23 \pm 0.39)\%$ [16], and $m_c/m_b = 0.29 \pm 0.02$ [3, 13]. There are also long distance resonance contributions to $B \rightarrow X_s \ell^+ \ell^-$, arising from $B \rightarrow K^{(*)} \psi^{(\prime)} \rightarrow K^{(*)} \ell^+ \ell^-$. These appear as an effective $(\bar{s}_L \gamma_\mu b_L)(\bar{\ell} \gamma_\mu \ell)$ interaction and are incorporated into C_9^{eff} via the modification $Y(\hat{s}) \rightarrow Y'(\hat{s}) \equiv Y(\hat{s}) + Y_{res}(\hat{s})$, where $Y_{res}(\hat{s})$ is given in Ref. [17]. These pole contributions lead to a significant interference between the dispersive part of the resonance and the short distance contributions. However, suitable cuts on the lepton pair mass spectrum can cleanly separate the short distance physics from the resonance contributions.

The operator basis for the decay $B \rightarrow X_s \gamma$ contains the first eight operators in the effective Hamiltonian of Eq. (1). The leading logarithmic QCD corrections to the decay width have been completely resummed, but lead to a sizeable μ dependence of the branching fraction (as demonstrated above with the large value of ΔC_7^{eff}), and hence it is essential to include the next-to-leading order corrections to reduce the theoretical uncertainty. In this case, the calculation of the perturbative QCD corrections involves several steps, requiring corrections to both the Wilson coefficients

and the matrix elements of the operators in Eq. (1) in order to ensure a scheme independent result. For the matrix elements, this includes the QCD bremsstrahlung corrections[18] $b \rightarrow s\gamma + g$, and the NLO virtual corrections which have recently been completed in both the NDR and 't Hooft-Veltman schemes [3]. Summing these contributions to the matrix elements and expanding them around $\mu = m_b$, one arrives at the decay amplitude

$$\mathcal{M}(b \rightarrow s\gamma) = -\frac{4G_F V_{tb} V_{ts}^*}{\sqrt{2}} D \langle s\gamma | \mathcal{O}_7(m_b) | b \rangle_{tree}, \quad (6)$$

with

$$D = C_7^{eff}(\mu) + \frac{\alpha_s(m_b)}{4\pi} \left(C_i^{(0)eff}(\mu) \gamma_{i7}^{(0)eff} \log \frac{m_b}{\mu} + C_i^{(0)eff} r_i \right). \quad (7)$$

Here, the quantities $\gamma_{i7}^{(0)eff}$ are the entries of the effective leading order anomalous dimension matrix, and the r_i are computed in Greub *et al.* [3], for $i = 2, 7, 8$. The first term in Eq. 7, $C_7^{eff}(\mu)$, must be computed at NLO precision, while it is consistent to use the leading order values of the other coefficients. The explicit logarithms $\alpha_s(m_b) \log(m_b/\mu)$ in the equation are cancelled by the μ dependence of $C_7^{(0)eff}(\mu)$. This feature significantly reduces the scale dependence of the resulting branching fraction. The contribution to the inclusive width including these virtual corrections is then

$$\Gamma_{NLO}^{virt}(B \rightarrow X_s \gamma) = \frac{m_{b,pole}^5 G_F^2 \alpha_{em} |V_{tb} V_{ts}^*|^2}{32\pi^4} F |D|^2, \quad (8)$$

where the factor $F = m_b^2(m_b)/m_{b,pole}^2 = 1 - 8\alpha_s(m_b)/3\pi$ arises from the mass factor present in the magnetic dipole operator. This should be compared to the familiar leading order result (which omits the virtual corrections to $\langle \mathcal{O}_7 \rangle$)

$$\Gamma(B \rightarrow X_s \gamma) = \frac{m_{b,pole}^5 G_F^2 \alpha_{em} |V_{tb} V_{ts}^*|^2 |C_7^{eff}(\mu)|^2}{32\pi^4}. \quad (9)$$

For the Wilson coefficients, the NLO result entails the computation of the $\mathcal{O}(\alpha_s)$ terms in the matching conditions, and the renormalization group evolution of the $C_i(\mu)$ must be computed using the $\mathcal{O}(\alpha_s^2)$ anomalous dimension matrix. The former step has been completed[19], but the latter step is quite difficult since some entries in the matrix have to be extracted from three-loop diagrams. Nonetheless, preliminary NLO results for these anomalous dimensions have recently been reported [5], with the conclusion being that in the NDR scheme the NLO correction to $C_7^{eff}(\mu)$ is small. Therefore, a good approximation for the inclusive width is obtained by employing the leading order expression for $C_7^{eff}(\mu)$, with the understanding that this introduces a small inherent uncertainty in the calculation.

The total inclusive width is then given by the sum of the virtual and bremsstrahlung corrections, $\Gamma(B \rightarrow X_s \gamma) = \Gamma^{virt} + \Gamma^{brems}$, where Γ^{brems} is given in Greub *et al.* [18, 3], and the branching fraction

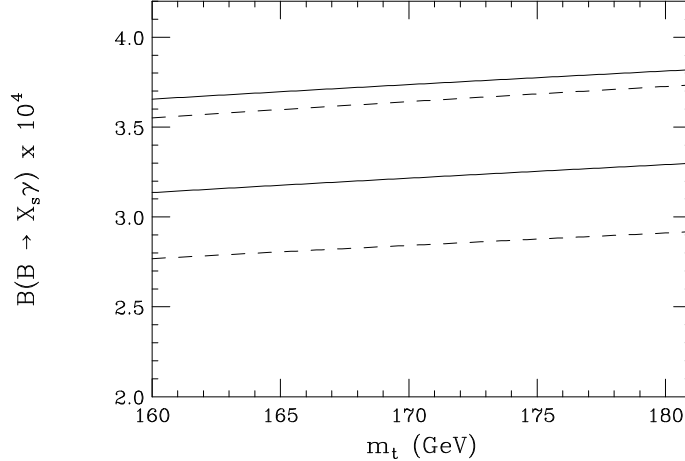


Figure 1: The branching ratio of $B \rightarrow X_s \gamma$ versus m_t . The dashed lines indicate the error in the branching ratio if we fix $\mu = m_b$ and vary all the other parameters over their allowed ranges: $\alpha_s(M_Z) = 0.118 \pm 0.003$, $B_{sl} = 10.23 \pm 0.39\%$, and $m_c/m_b = 0.29 \pm 0.02$. The solid lines indicate the error for $m_b/2 < \mu < 2m_b$ and all other parameters fixed to their central values.

is calculated by scaling to the semi-leptonic decay rate. The leading order power corrections in the heavy quark expansion are identical for $B \rightarrow X_s \gamma$ and $B \rightarrow X \ell \nu$, and hence cancel in the ratio [20]. This allows us to approximate $\Gamma(B \rightarrow X_s \gamma)$ with the perturbatively calculable free quark decay rate. For $m_t^{phys} = 175 \pm 6$ GeV, $m_b/2 \leq \mu \leq 2m_b$, $\alpha_s = 0.118 \pm 0.003$, $B_{sl} = (10.23 \pm 0.39)\%$, and $m_c/m_b = 0.29 \pm 0.02$, we find the branching fraction

$$B(B \rightarrow X_s \gamma) = (3.25 \pm 0.30 \pm 0.40) \times 10^{-4}, \quad (10)$$

where the first error corresponds to the combined uncertainty associated with the value of m_t and μ , and the second error represents the uncertainty from the other parameters. This is well within the range observed by CLEO. In Fig. 1 we display our results for $B(B \rightarrow X_s \gamma)$ as a function of the top mass. The dashed lines indicate the error in the branching ratio if we fix $\mu = m_b$ and vary all the other parameters over their allowed ranges given above. The solid lines indicate the error for $m_b/2 < \mu < 2m_b$ with all other parameters fixed to their central values. This visually demonstrates that the error in the theoretical calculation of $B \rightarrow X_s \gamma$ is not overwhelmed by the scale uncertainty; other uncertainties are now comparable.

Measurements of $B(B \rightarrow X_s \gamma)$ alone constrain the magnitude, but not the sign, of $C_7^{eff}(\mu)$. We can write the coefficients at the matching scale in the form $C_i(M_W) = C_i^{SM}(M_W) + C_i^{new}(M_W)$, where $C_i^{new}(M_W)$ clearly represents the contributions from new interactions. Due to operator mixing, $B \rightarrow X_s \gamma$ then limits the possible values for $C_i^{new}(M_W)$ for $i = 7, 8$. These bounds are summarized in Fig. 2. Here, the solid bands correspond to the constraints obtained from the current CLEO

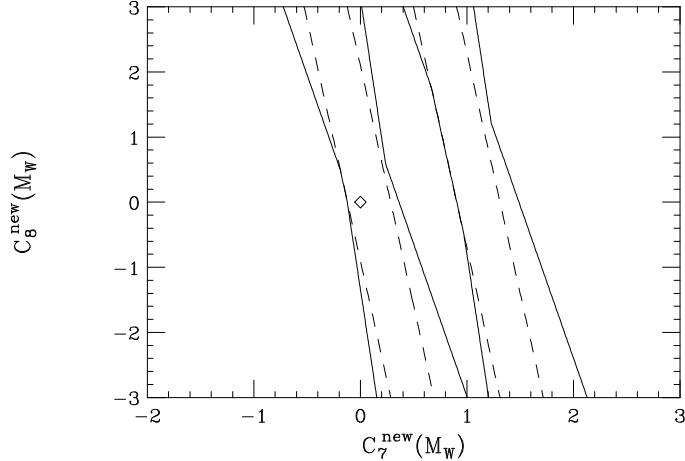


Figure 2: Bounds on the contributions from new physics to $C_{7,8}$. The region allowed by the CLEO data corresponds to the area inside the solid diagonal bands. The dashed bands represent the constraints when the renormalization scale is set to $\mu = m_b$. The diamond at the position (0,0) represents the standard model.

measurement, taking into account the variation of the renormalization scale $m_b/2 \leq \mu \leq 2m_b$, as well as the allowed ranges of the other input parameters. The dashed bands represent the constraints when the scale is fixed to $\mu = m_b$. We note that large values of $C_8^{new}(M_W)$ are allowed even in the region where $C_7^{new}(M_W) \simeq 0$. Experimental bounds on the decay $b \rightarrow sg$ are needed to constraint C_8 .

Measurement of the kinematic distributions associated with the final state lepton pair in $B \rightarrow X_s \ell^+ \ell^-$ as well as the rate for $B \rightarrow X_s \gamma$ allows for the determination of the sign and magnitude of all the Wilson coefficients for the contributing operators in a model independent fashion [9, 10]. Here, we perform a Monte Carlo analysis in order to ascertain how much quantitative information will be obtainable at future B -factories. We improve upon our previous study[10] by implementing the NLO computations for these decays and by examining the luminosity dependence of the resulting global fits. For the process $B \rightarrow X_s \ell^+ \ell^-$, we consider the lepton pair invariant mass distribution and forward-backward asymmetry for $\ell = e, \mu, \tau$, and the tau polarization asymmetry for $B \rightarrow X_s \tau^+ \tau^-$. We note that the asymmetries have the form $A(\hat{s}) \sim C_{10}(\text{Re} C_9^{eff} f_1(\hat{s}) + C_7^{eff} f_2(\hat{s}))$, and hence are sensitive probes of the Wilson coefficients. We generate “data,” assuming the SM is realized, by dividing the lepton pair invariant mass spectrum into nine bins. Six of the bins are taken to be in the low dilepton invariant mass region below the J/ψ resonance (in order to take advantage of the larger statistics), with $0.02 \leq \hat{s} \leq 0.32$ and a bin width of $\Delta \hat{s} = 0.05$. We have also cut out the region near $q^2 = 0$ in order to remove the photon pole. The high $M_{\ell^+ \ell^-}$ region above the ψ' pole

is divided into three bins, corresponding to $0.6 \leq \hat{s} \leq 0.7$, $0.7 \leq \hat{s} \leq 0.8$, and $0.8 \leq \hat{s} \leq 1.0$. The number of events per bin is calculated as

$$N_{bin} = \mathcal{L} \int_{\hat{s}_{min}}^{\hat{s}_{max}} \frac{d\Gamma(B \rightarrow X_s \ell^+ \ell^-)}{d\hat{s}} d\hat{s}, \quad (11)$$

and the average value of the asymmetries in each bin is

$$\langle A \rangle_{bin} = \frac{\mathcal{L}}{N_{bin}} \int_{\hat{s}_{min}}^{\hat{s}_{max}} A \frac{d\Gamma(B \rightarrow X_s \ell^+ \ell^-)}{d\hat{s}} d\hat{s}. \quad (12)$$

We statistically fluctuate the “data” using a normalized Gaussian distributed random number procedure, where the statistical errors are given by $\delta N = \sqrt{N}$ and $\delta A = \sqrt{(1 - A^2)/N}$. We expect the errors in each bin to be statistics dominated and hence we neglect any possible systematic errors. For $B \rightarrow X_s \gamma$, we again statistically fluctuate the “data” for the inclusive rate. However, in this case, the statistical precision will eclipse the possible systematic and theoretical accuracy. We thus assume a flat 10% error in the determination of the branching fraction in anticipation of future theoretical and experimental improvements. A three dimensional χ^2 fit to the coefficients $C_{7,9,10}(\mu)$ is performed, employing the usual prescription

$$\chi_i^2 = \sum_{bins} \left(\frac{Q_i^{obs} - Q_i^{SM}}{\delta Q_i} \right)^2, \quad (13)$$

for each observable quantity Q_i . We repeat this procedure for three values of the integrated luminosity, 3×10^7 , 10^8 , and 5×10^8 $B\bar{B}$ pairs, corresponding to the expected e^+e^- B -factory luminosities of one year at design, one year at an upgraded accelerator, and the total accumulated luminosity at the end of the programs. Hadron colliders will, of course, also contribute to this program, but it is more difficult to assess their potential systematic and statistical weights without further study.

The 95% C.L. allowed regions as projected onto the $C_9(\mu) - C_{10}(\mu)$ and $C_7^{eff}(\mu) - C_{10}(\mu)$ planes are depicted in Figs. 3(a-b), where the diamond represents the expectations in the SM. We see that the determinations are relatively poor for 3×10^7 $B\bar{B}$ pairs and that higher statistics are required in order to focus on regions centered around the SM. Clearly, C_9 and C_{10} are highly correlated, whereas C_7^{eff} and C_{10} are not. We see that the sign, as well as the magnitude, of all the coefficients including C_7^{eff} can now be determined.

For the remainder of this paper, we analyze the supersymmetric contributions to the Wilson coefficients in terms of the quantities

$$R_i \equiv \frac{C_i^{susy}(M_W)}{C_i^{SM}(M_W)} - 1 \equiv \frac{C_i^{new}(M_W)}{C_i^{SM}(M_W)}, \quad (14)$$

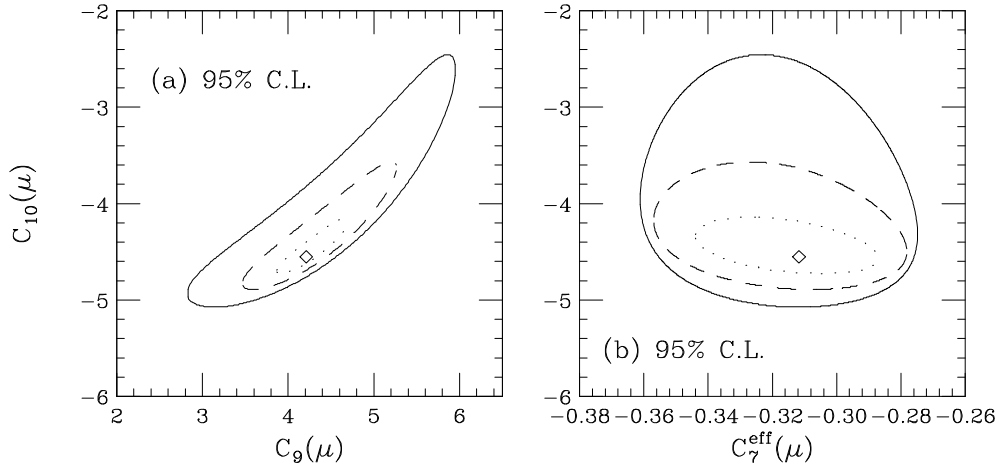


Figure 3: The 95% C.L. projections in the (a) $C_9 - C_{10}$ and (b) $C_7^{eff} - C_{10}$ planes, where the allowed regions lie inside of the contours. The solid, dashed, and dotted contours correspond to 3×10^7 , 10^8 , and 5×10^8 $B\bar{B}$ pairs. The SM prediction is labeled by the diamond.

where $C_i^{susy}(M_W)$ includes the full standard model plus superpartner contributions. R_i is meant to indicate a relative fraction difference from the standard model value. It is most convenient to define these ratios at the W scale to avoid the added complication of the renormalization group evolution to the low scale.

3 Expectations in supersymmetry

Supersymmetry has many potential sources for flavor violation. The flavor mixing angles among the squarks are *a priori* separate from the CKM angles of the standard model quarks. If we allow the super-CKM angles to be arbitrary then we find, for example, that the relative SUSY versus SM amplitudes for $b \rightarrow s$ are $(M_W/\tilde{m})^n (\tilde{V}_{ts}^* \tilde{V}_{tb} / V_{ts}^* V_{tb})$. $|V_{ts}^* V_{tb}| \simeq 0.04$, and so allowing the \tilde{V} angles to be oriented randomly with respect to the CKM angles constitutes a flavor problem for supersymmetry if \tilde{m} is near the weak scale. Natural solutions to this problem exist. One solution is alignment [21] of the super-CKM matrices with the quark matrices. Another natural solution is universality induced by gauge mediated supersymmetry breaking [22]. In the minimal model of gauge mediated supersymmetry breaking [23], the $b \rightarrow s\gamma$ decay is currently not a strong constraint on the spectrum, but will show deviations from the standard model at the B -factory if $m_{\tilde{\chi}_1^\pm} \lesssim 350$ GeV. We adopt the viewpoint in this paper that flavor-blind (diagonal) soft terms [24] at the high scale are the phenomenological source for the soft scalar masses at the high scale, and that the CKM angles are the only relevant flavor violating sources. We build on other studies of

supersymmetry effects on rare B decays [25, 9, 26].

The spectroscopy of the supersymmetric states is model dependent. We will analyze two possibilities. The first possibility is that all the supersymmetric states follow from common scalar mass at high scale and common gaugino mass at the high scale. This is the familiar minimal supergravity model. The second possibility is to relax the condition of common scalar masses at the high scale and allow them to take on more uncorrelated values at the low scale while still preserving gauge invariance.

We begin by searching over the full parameter space of minimal supergravity model. We use the words “minimal supergravity” as an idiom to indicate that we generate [27] these models by applying common soft scalar masses and common gaugino masses at the boundary scale. The triscalar A terms are also an input at the high scale and are universal. The radiative electroweak symmetry breaking conditions yield the B and μ^2 terms as output, with a $\text{sign}(\mu)$ ambiguity left over as an input parameter. (Here μ refers to the Higgsino mixing parameter.) We also choose $\tan\beta$ and restrict it to a range which will yield perturbative Yukawa couplings up to the GUT scale.

We have generated thousands of solution according to the above procedure. The ranges of our input parameters are $0 < m_0 < 500 \text{ GeV}$, $50 < m_{1/2} < 250 \text{ GeV}$, $-3 < A_0/m_0 < 3$, $2 < \tan\beta < 50$, and we have taken $m_t^{phys} = 175 \text{ GeV}$. Each supersymmetric solution is kept only if it is not in violation with present constraints from SLC/LEP and Tevatron direct sparticle production limits. For each of these remaining solutions we now calculate R_{7-10} [28]. Expansions of $C_i(M_W)$ with the assumption of approximate universality are given in the appendix.

First, we present a scatter plot of R_7 vs. R_8 in Fig. 4; we remind the reader that these quantities are evaluated at the electroweak scale. Again, each point in the scatter plot is derived from the minimal supergravity model with different initial conditions. Also, each point is consistent with all collider bounds and is out of reach of LEP II. The first thing to note from the figure is that large values of R_7 and R_8 are generated, and the R_7 and R_8 values are very strongly correlated. The diagonal bands represent the bounds on the Wilson coefficients from the observation of $B \rightarrow X_s \gamma$ as determined in the previous section. We note that these bands appear to be straight here as they correspond to a small region of Fig. 2. We see that the current CLEO data already places significant restrictions on the supersymmetric parameter space. Further constraints will be obtainable once a 10% measurement of $B(B \rightarrow X_s \gamma)$ is made, and the sign of C_7 is determined from a global fit described in the previous section. In this case, if no deviations from the SM are observed, the supersymmetric contributions will be restricted to lie in the dashed band. It is clear that these processes can explore vast regions of the supersymmetric parameter space. In fact, it is possible that spectacularly large deviations in rare B decays could be manifest at B factories, while collider

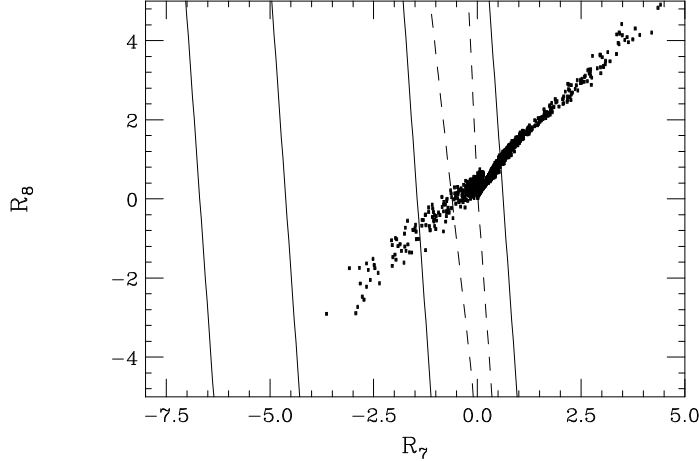


Figure 4: Parameter space scatter plot of R_7 vs. R_8 in minimal supergravity model. The allowed region from CLEO data, as obtained in Fig. 2, lies inside the 2 sets of solid diagonal bands. The dashed band represents the potential 10% measurement from the previously described global fit to the coefficients.

experiments would not detect a hint of new physics.

The large effects in R_7 and R_8 are coming from models with $|\mu| \lesssim 400$ GeV as can be seen in Fig. 5. This is because light charged Higgsinos, or rather light charginos with a large Higgsino fraction, are required in order to yield a large effect on the Wilson coefficients. Later in this section we will demonstrate this requirement more carefully by expanding the supersymmetric contributions in the Higgsino limit.

In Fig. 6 the correlation between R_9 and R_{10} is plotted using the same supersymmetric parameter space. We see that R_9 is always positive since charged Higgs and chargino contributions always add constructively. We see that the values of R_9 and R_{10} are bounded by about 0.04, a small number compared to the range for R_7 . The main reason for these smaller values is the dependence on the bottom Yukawa $\lambda_b \propto 1/\cos\beta$. R_7 has a contribution directly dependent on this $1/\cos\beta$ Yukawa enhancement, and the other multiplicative terms associated with this Yukawa are the large top Yukawa and a large kinematic loop factor. R_9 and R_{10} do not have such factors due the chirality structure of these operators and the requirement that leptons and sleptons only couple via $SU(2)$ and $U(1)$ gauge couplings. These factors, along with the correlations between the mass spectra dictated by minimal supergravity relations, render the minimal supergravity contributions to $R_{9,10}$ essentially unobservable. The solid lines in this figure correspond to the 95% C.L. bounds obtainable with high integrated luminosity (5×10^8 $B\bar{B}$ pairs) at B factories from the global fit performed in the previous section. If large deviations in $R_{9,10}$ are observed, then, of course, that would be

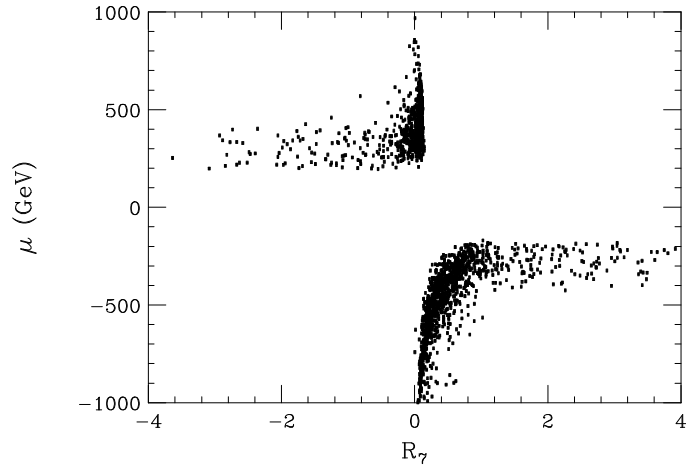


Figure 5: Parameter space scatter plot of R_7 vs. μ in minimal supergravity model.

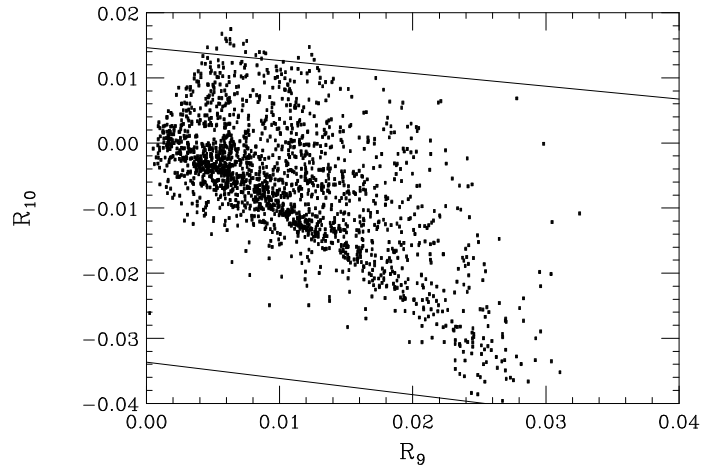


Figure 6: Parameter space scatter plot of R_9 vs. R_{10} in minimal supergravity model. The global fit to the coefficients obtained in Fig. 3 with $5 \times 10^8 B\bar{B}$ pairs corresponds to the region inside the diagonal bands.

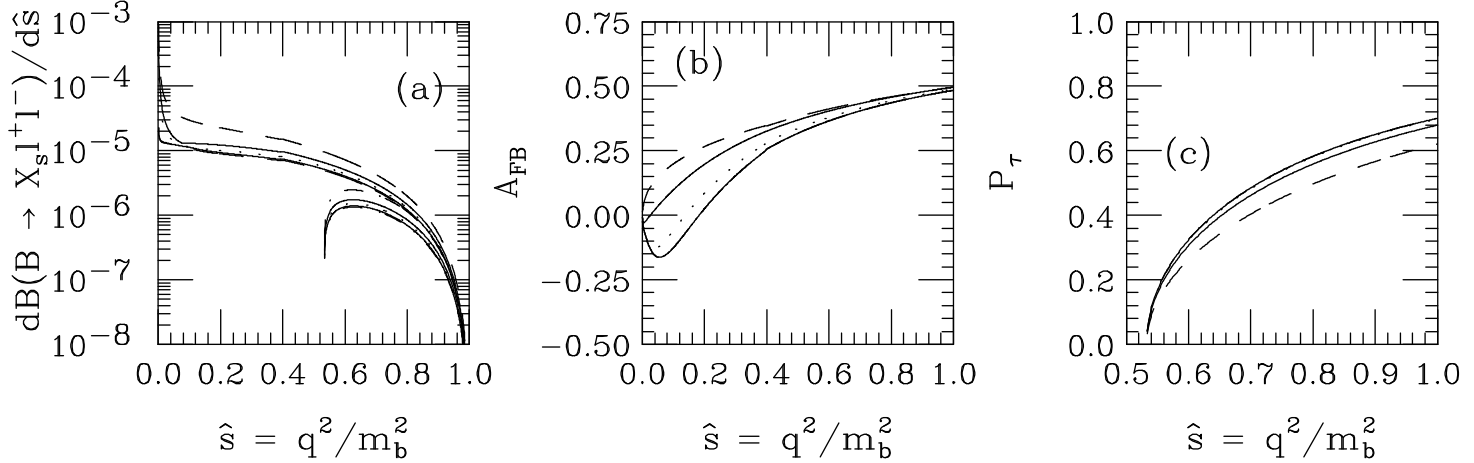


Figure 7: The (a) differential branching fraction, (b) lepton pair forward-backward asymmetry, and (c) tau polarization asymmetry as a function of the scaled momentum transfer to the lepton pair, $\hat{s} \equiv q^2/m_b^2$. The dotted curves represent the SM prediction, while the dashed and solid bands correspond to the maximal potential deviations due to supersymmetric contributions for different regions of the parameter space as described in the text. In some cases the dashed line overlaps with the solid line.

an indication that the minimal model presently under discussion is not the correct description of nature. Later in this section we will find that even when the mass correlations of the minimal supergravity model are lifted, the quantities $R_{9,10}$ still cannot be large.

We next examine the effects of the minimal supergravity model on the kinematic distributions for $B \rightarrow X_s \ell^+ \ell^-$. Using our generated models as input, we calculate the maximal deviations from the SM for the $M_{\ell^+ \ell^-}$ distribution, lepton pair forward-backward asymmetry, and tau polarization asymmetry. These are displayed in Figs. 7(a-c). Here, the dotted line corresponds to the SM prediction, while the dashed (solid) bands represent the maximal possible deviations due to points in the supersymmetric parameter space which are within (outside) the expected reach of LEP II. We have also demanded consistency with the present CLEO data on $B \rightarrow X_s \gamma$. We see from the figure that, generally, larger deviations are expected for the asymmetries than for the branching fraction, and that constraints from LEP II on supersymmetry greatly affect the magnitude of these potential deviations. Since the SUSY contributions to $R_{9,10}$ are so small these deviations are mainly due to $R_{7,8}$. We find that much larger effects in these distributions are possible if the constraint from radiative B decays is not taken into account.

We now adopt a more phenomenological approach. The maximal effects for the parameters R_i can be estimated for a superparticle spectrum independent of these high scale assumptions. However, we still maintain the assumption that CKM angles alone constitute the sole source of

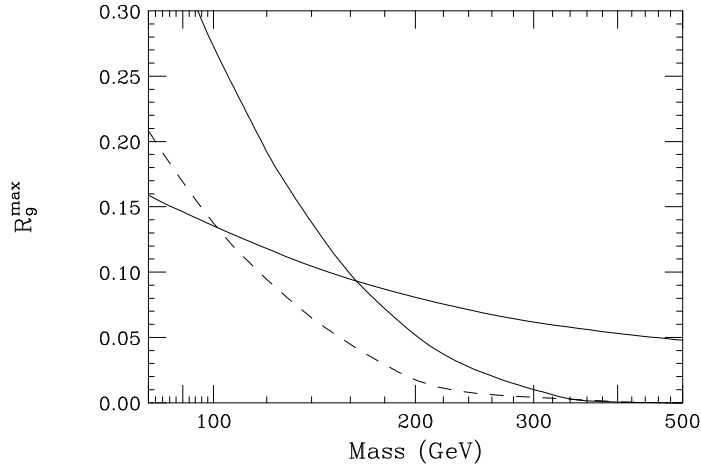


Figure 8: The maximum value of $R_9 = C_9^{susy}(M_W)/C_9^{SM}(M_W) - 1$ achievable for general supersymmetric models. The top solid line comes from $t - H^\pm$ contribution and is displayed versus the H^\pm mass. The bottom solid line is from $\tilde{t}_i - \chi_j^\pm$ contribution with $\tan\beta = 1$ and is shown versus the χ_i^\pm mass. The dashed line is the $\tilde{t}_i - \chi_j^\pm$ contribution with $\tan\beta = 2$. The other mass parameters which are not plotted are chosen to be just above LEP II and Tevatron's reach.

flavor violations in the full supersymmetric lagrangian. We will focus on the region $\tan\beta \lesssim 30$ since enormous effects are possible in the large $\tan\beta$ limit; later on we will discuss the large $\tan\beta$ limit more carefully. The most important features which result in large effects are a light \tilde{t}_1 state present in the spectrum and at least one light chargino state. For the dipole moment operators a light Higgsino is most important. A pure higgsino and/or pure gaugino state have less of an effect than two mixed states when searching for maximal effects in C_9 and C_{10} . In fact, we have found that $M_2 \simeq 2\mu$ is optimal.

Fig. 8, and 9 display the maximum contribution to $R_{9,10} = C_{9,10}^{susy}(M_W)/C_{9,10}^{SM}(M_W) - 1$ versus an applicable SUSY mass scale. The other masses which are not plotted (\tilde{t}_i, \tilde{l}_L , etc.) are chosen to be just above the reach of LEP II or the Tevatron, whichever gives better bounds.

The maximum size of $R_{9,10}$ is much larger than what was allowed in the minimal supergravity model. The reason for this is the lifted restriction on mass correlations. Light sleptons, sneutrinos, charginos, and stops are allowed simultaneously with mixing angles giving the maximal contribution to the R_i 's. However, we find that the maximum allowed values for $R_{9,10}$ are still much less than unity. Earlier we determined that B factory data would be sensitive to $\Delta R_9 \gtrsim 0.3$ and $\Delta R_{10} \gtrsim 0.08$ at the highest luminosities, and so the largest SUSY effect would give a $1 - 2\sigma$ signal in $R_{9,10}$, hardly enough to be a compelling indication of physics beyond the standard model. If, on the other hand, much larger deviations of $R_{9,10}$ are found in the data, it could mean the assumption of only CKM angles allowed in the supersymmetric lagrangian is inaccurate, or it could indicate that

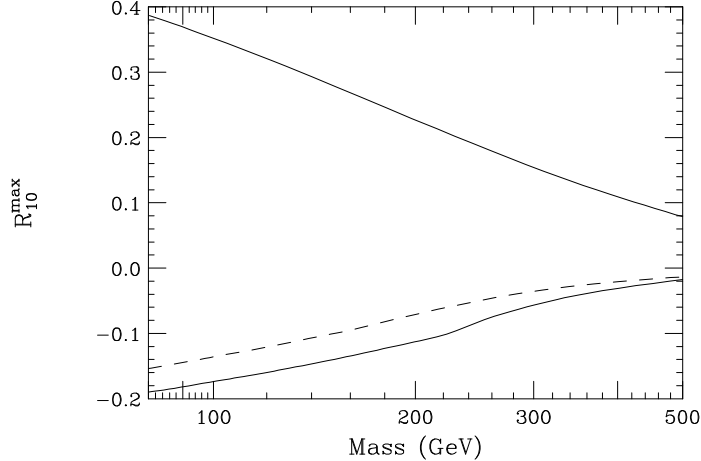


Figure 9: The maximum value of $R_{10} = C_{10}^{susy}(M_W)/C_{10}^{SM}(M_W) - 1$ achievable for general supersymmetric models. The top solid line comes from $t - H^\pm$ contribution and is shown versus the H^\pm mass. The bottom solid line is from $\tilde{t}_i - \chi_j^\pm$ contribution with $\tan\beta = 1$ and is plotted versus the χ_i^\pm mass. The dashed line is the $\tilde{t}_i - \chi_j^\pm$ contribution with $\tan\beta = 2$. The other mass parameters which are not presented are chosen to be just above LEP II and Tevatron's reach.

minimal supersymmetry is not the source of physics beyond the standard model.

It should be remembered that even though it appears difficult to resolve the SUSY contributions to the coefficients C_{9-10} , the $B \rightarrow X_s l^+ l^-$ decay rate and distributions can still demonstrate large deviations from the standard model induced largely by the SUSY corrections to $C_7(M_W)$. The global fit using all the rare B decay data is still necessary in this circumstance since it will enable a precise determination in which band in the C_7 vs. C_8 plot we reside. Furthermore, some ideas [29] of physics beyond the standard model predict small corrections to $B \rightarrow X_s \gamma$ and large deviations in $B \rightarrow X_s l^+ l^-$, motivating again the procedure of doing a global fit to all the rare B decay data.

Given the sensitivity of all the observables it is instructive to narrow the focus to $C_7(M_W)$. In the minimal supergravity models, the scalars obtain dependence on the gaugino masses through the renormalization group running. However, the gaugino masses do not get substantial scalar mass contributions to their masses. This tends to separate the mass scale for the scalars far from the gauginos. The separation is especially important between electroweak gauginos and strongly interacting squarks. Neglecting the D-term contributions the squarks have masses given roughly by $\tilde{m}_q^2 \approx m_0^2 + 7m_{1/2}^2$ and the weak gaugino has mass $m_{\tilde{W}} \approx 0.8m_{1/2}$ where m_0 is the common scalar mass and $m_{1/2}$ is the common gaugino mass at the high scale. From these equations it is easy to see that the squark masses are much heavier than the weak gaugino mass for any given $m_{1/2}$ and m_0 .

When all the squark masses are very heavy (much heavier than the charginos, for example) then

the SUSY contributions to $C_7(M_W)$ decouple. However, one eigenvalue of the stop squark mass matrix might be much lighter than the other squarks. The large top Yukawa tends to drive \tilde{t}_R much lower than the other $\tilde{q}_{L,R}$. Also, the stop squark has a mixing term proportional to $m_t(A_t - \mu \cot \beta)$. Since this mixing is proportional to the top mass, it can be substantial. Mixings in any positive definite matrix will push the lightest eigenvalue lower and the heaviest eigenvalue higher. These two effects tend to push the lightest stop eigenvalue well below the other squarks. In fact, a highly mixed, light stop squark is generic in these theories. For a large supersymmetric contribution to R_b [30] and/or the ability to achieve successful baryogenesis in the early universe [31], a light \tilde{t}_R is needed. We would therefore like to present results on $C_7(M_W)$ in the limit of one light squark, namely the \tilde{t}_1 , and light charginos. We allow the \tilde{t}_1 to have arbitrary components of \tilde{t}_L and \tilde{t}_R since cross terms can become very important. This is especially noteworthy in the high $\tan \beta$ limit as we will discuss below.

In this limit of one light top squark, we can expand the chargino-stop contribution to $C_7(M_W)$ as

$$\delta C_7(M_W) = \frac{1}{6} \sum_i \frac{M_W^2}{m_{\chi_i^\pm}^2} \lambda_i^L \left\{ \lambda_i^L F(x_i) + 2\lambda_i^R \frac{m_{\chi_i^\pm}}{m_b} J(x_i) \right\}, \quad (15)$$

where

$$\begin{aligned} \lambda_i^L &= -T_{11}V_{i1} + T_{12} \frac{V_{i2}}{\sqrt{2}} \frac{m_t}{M_W} \frac{1}{\sin \beta}, \\ \lambda_i^R &= T_{11} \frac{U_{i2}}{\sqrt{2}} \frac{m_b}{M_W} \frac{1}{\cos \beta}, \\ x_i &= \frac{m_{\tilde{t}_1}^2}{m_{\chi_i^\pm}^2}, \\ J(x) &= \frac{5-7x}{2(1-x)^2} + \frac{2x-3x^2}{(1-x)^3} \log x, \\ F(x) &= \frac{7-5x-8x^2}{6(1-x)^3} + \frac{2x-3x^2}{(1-x)^4} \log x. \end{aligned}$$

The matrix T_{ij} is the stop mixing matrix which rotates $(\tilde{t}_L, \tilde{t}_R)$ into $(\tilde{t}_1, \tilde{t}_2)$. The matrices U_{ij} and V_{ij} are the usual chargino mixing matrices [32]. For the reader's convenience we have plotted the functions $F(x)$ and $J(x)$ in Fig. 10.

The total contribution to $\delta C_7(M_W)$ above will depend on several combinations of mixing angles: T_{11}^2 , $T_{11}T_{12}$, $V_{11}U_{12}$, etc, and cancellations can occur for different signs of μ [34]. Therefore, it is instructive to summarize the relative signs of each angle combination in the evaluation of Eq. 15:

$$\text{sgn}(U_{12}V_{11}) = -\text{sgn}(\mu),$$

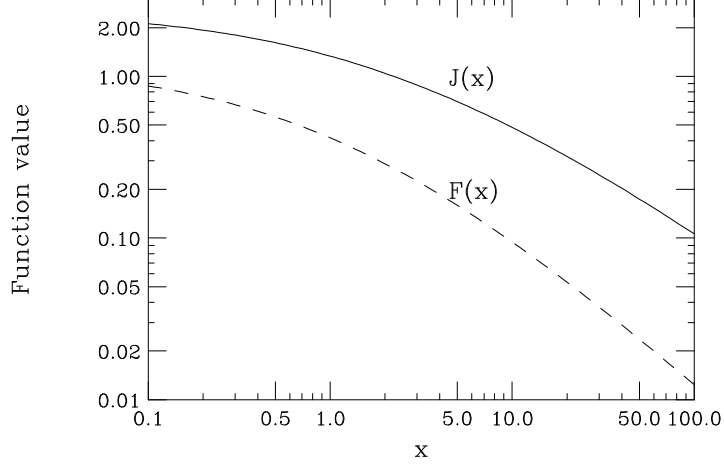


Figure 10: The kinematic loop functions $F(x)$ and $J(x)$ necessary to calculate the standard model and supersymmetric contributions to $C_7(M_W)$. $J(x)$ and $F(x)$ asymptote to $5/2$ and $7/6$ respectively as $x \rightarrow 0$.

$$\begin{aligned}
 \text{sgn}(U_{12}V_{12}) &= +\text{sgn}(\mu), \\
 &\quad +, \text{ if } M_2 \tan \beta + \mu < 0, \\
 \text{sgn}(V_{11}V_{12}) &= -\text{sgn}(M_2 \tan \beta + \mu), \\
 \text{sgn}(T_{11}T_{12}) &= +, \text{ if } \tilde{t}_R < \tilde{t}_L \text{ and } A_t - \mu \cot \beta < 0, \\
 &\quad -, \text{ if } \tilde{t}_R < \tilde{t}_L \text{ and } A_t - \mu \cot \beta > 0, \\
 &\quad -, \text{ if } \tilde{t}_L < \tilde{t}_R \text{ and } A_t - \mu \cot \beta < 0, \\
 &\quad +, \text{ if } \tilde{t}_L < \tilde{t}_R \text{ and } A_t - \mu \cot \beta > 0.
 \end{aligned}$$

We are using the Haber-Kane convention for the sign of μ which requires, for example, that $+\mu$ be in the chargino mass matrix.

The first case we discuss is the limit where the lightest chargino is a pure Higgsino and the lightest stop is pure right-handed: $\chi_1^\pm \sim \tilde{H}^\pm$, $\tilde{t}_1 \sim \tilde{t}_R$. Then Eq. 15 can be written as

$$\delta C_7(M_W) = \frac{1}{12} \frac{m_t^2}{m_{\chi_1^\pm}^2} F\left(\frac{m_{\tilde{t}_1}^2}{m_{\chi_1^\pm}^2}\right). \quad (16)$$

This limit is roughly applicable in the case where R_b is affected substantially by supersymmetric corrections [30, 33]. After LEP II completes its run the charginos will have been probed up to about M_W , and so the maximum effect on $\delta C_7(M_W)$ that would be possible in this limit (if LEP II does not find charginos) corresponds to setting $m_{\chi_1^\pm} \simeq M_W$. We do this and show the result as a function of the \tilde{t}_R mass in Fig. 11 (dashed line). The contribution to $C_7(M_W)$ in this limit is always

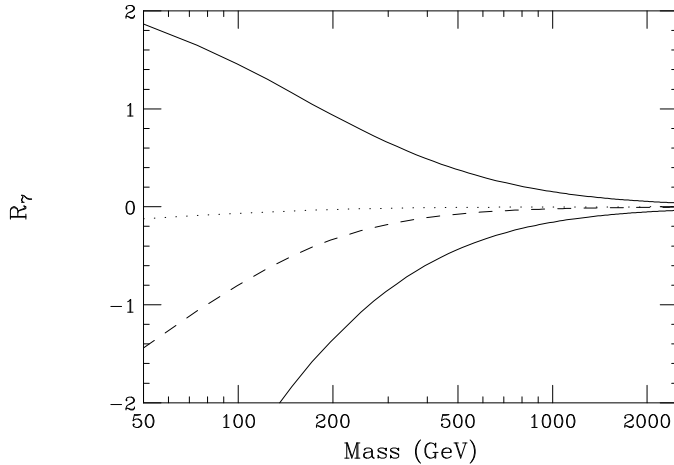


Figure 11: Contributions to R_7 in different limits. The top solid line is the charged H^\pm/t contribution versus m_{H^\pm} . The bottom solid line is the $\tilde{\chi}_1^\pm/\tilde{t}_1$ contribution versus $m_{\tilde{\chi}^\pm}$ where both the chargino and stop are maximally mixed states (equal magnitude mixtures for all states). This line was made for $\mu < 0$. The dashed line is the $\tilde{H}^\pm/\tilde{t}_R$ contribution, and the dotted line is the $\tilde{W}^\pm/\tilde{t}_1$ contribution ($\tilde{t}_1 \propto \tilde{t}_R + \tilde{t}_L$ is a maximally mixed stop mass eigenstate). These two lines are both plotted against the $\tilde{\chi}_1^\pm$ mass. All lines are for $\tan\beta = 2$ and $m_t = 175$ GeV. We have set all other masses to be just above the reach of LEP II.

positive. Since $C_7^{SM}(M_W)$ is a negative quantity in our convention, then $R_7 = \delta C_7(M_W)/C_7^{SM}(M_W)$ is necessarily negative as well.

In the case where the only light chargino is a pure Wino we find,

$$\delta C_7(M_W) = \frac{T_{11}^2}{6} \frac{m_W^2}{m_{\tilde{W}}^2} F\left(\frac{m_{\tilde{t}_1}^2}{m_{\tilde{W}}^2}\right). \quad (17)$$

If μ is very large and $\tan\beta$ is not too large, then this contribution will be the largest to $\delta C_7(M_W)$. The effects of a light pure Wino are generally small since the Wino couples like g_2 rather than the top Yukawa, and since generally supersymmetric models do not yield light \tilde{t}_L necessary to couple with the Wino. The loop integral $F(x)$ which characterizes the pure gaugino contribution is also small. Therefore, these contributions are both coupling suppressed and “loop integral” suppressed. The contribution of a pure Wino to R_7 is shown in Fig. 11 (dotted line). As expected, this contribution is rather small and always negative.

As we pointed out above, in minimal supergravity models, what we mostly expect is a highly mixed \tilde{t}_1 state such that all entries in the T_{ij} are filled. By just looking at the limit of pure \tilde{t}_R some very interesting effects can be missed. For example, an attractive high scale theory is supersymmetric $SO(10)$. These have been shown to successfully recover many important features of the standard model: quark to lepton ratios, CKM angles, etc. One of the generic predictions in

these models is that $\tan \beta$ must be rather high ($\sim m_t/m_b$) in order to get the b - τ - t mass unification. Therefore, it is interesting to focus on contributions to $C_7(M_W)$ which are especially dependent on high $\tan \beta$. Since $\lambda_i^R \propto 1/\cos \beta \sim \tan \beta$, we isolate this piece. For simplicity we expand about $\chi_{\tilde{1}}^\pm \sim \tilde{H}^\pm$, although it is clear that substantial contributions exist even if the chargino is not a pure Higgsino. We then obtain

$$\delta C_7 \simeq \text{sgn}(\mu) \frac{1}{6} \frac{m_t}{m_{\tilde{H}^\pm}} T_{11} T_{12} \tan \beta J \left(\frac{m_{\tilde{t}_1}^2}{m_{\tilde{H}^\pm}^2} \right). \quad (18)$$

Here it is crucial that there be substantial \tilde{t}_R and \tilde{t}_L contributions to \tilde{t}_1 . As argued above, this is generic in minimal supergravity theories. This expansion demonstrates that large $\tan \beta$ solutions ($\tan \beta \gtrsim 40$) can yield greater than $\mathcal{O}(1)$ contributions to R_7 for mass scales of 1 TeV. Even rather low values of $\tan \beta$ exhibit enhancements with a light Higgsino and light mixed stop. This is demonstrated for $\tan \beta = 2$ in Fig. 11 (solid line). Furthermore, large contributions are possible in both the negative and positive directions of R_7 depending on the sign of μ . For example, with $m_{\tilde{t}_1} = 250$ GeV, $|T_{11} T_{12}| = 1/10$, $m_{\tilde{\chi}_1^\pm} = 250$ GeV and $\tan \beta = 50$ we find that $|R_7(M_W)| \gtrsim 3$. Again, we are in a region of parameter space which is not tuned just to give this large effect in $B \rightarrow X_s \gamma$, rather we are in a region which is highly motivated by $SO(10)$ grand unified theories. The finite corrections to the b quark mass [35, 36] constitute approximately a 20% correction to the b Yukawa coupling when $\tan \beta \gtrsim 40$. This b Yukawa coupling is implicitly present in λ_i^R . Depending on the sign of μ this correction can be positive or negative. We don't include these finite b mass corrections in our analysis since it requires a detailed knowledge of the sparticle spectrum which we are not specifying.

The chirality structure of the O_i operators allow a large $\tan \beta$ enhancement only for the $C_{7,8}(M_W)$ coefficients. In O_7 the b_R quark must undergo an helicity flip as long as we neglect m_s dependent effects. Therefore, all contributions to C_7 in the standard model and MSSM must be proportional to the b -quark mass. However, some diagrams with $\tilde{t}_k/\tilde{\chi}_j^\pm$ loops allow proportionality to the bottom Yukawa alone, which yields a $m_b/\cos \beta$ enhancement for large $\tan \beta$ [37]. The mixings between the charged Higgs weak eigenstate and goldstone forbid $m_b/\cos \beta$ enhancements in the physical charged Higgs graphs. Furthermore, the helicity structure of the four-fermion operators $O_{9,10}$ forbid large $\tan \beta$ enhancements.

We conclude our analysis by examining the charged Higgs contributions to $B \rightarrow X_s \gamma$ alone. It is well-known [38, 39] that a H^\pm boson can contribute significantly to $C_{7,8}$, but has a smaller effect on the coefficients $C_{9,10}$; this is also illustrated above in Figs. 8,9,11. The form of the coefficients of the magnetic dipole operators in this case are presented in the appendix. From these equations, we see that not only do large enhancements occur for small values of $\tan \beta$, but more importantly, the

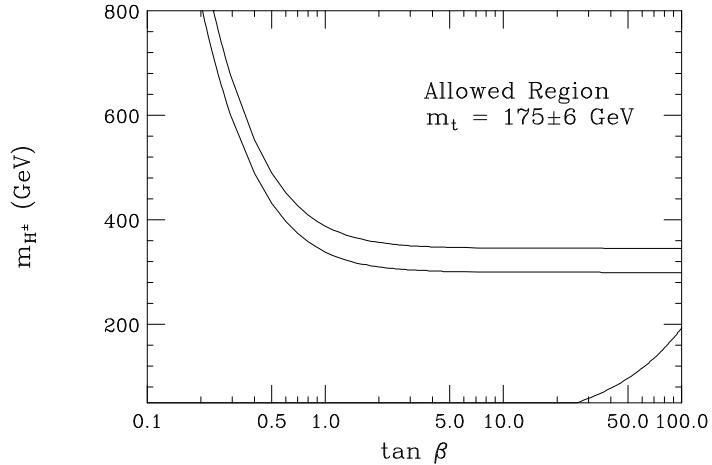


Figure 12: Constraints in the charged Higgs mass – $\tan\beta$ plane from the CLEO bound on $B(B \rightarrow X_s\gamma)$. The excluded region is that to the left and below the curves. The top line is for $m_t^{phys} = 181$ GeV and the bottom line is for $m_t^{phys} = 169$ GeV. We also display the restriction $\tan\beta/m_{H^\pm} > 0.52 \text{ GeV}^{-1}$ which arises from measurements of $B \rightarrow X\tau\nu$ as discussed in [40].

coefficients are always larger than those of the SM, independent of the value of $\tan\beta$. This leads to the familiar bound $m_{H^\pm} > 260$ GeV obtained from the measurement of $B(B \rightarrow X_s\gamma)$ by CLEO. However, this constraint does not make use of the recent NLO calculation of the matrix elements for this decay which are discussed in previous sections. We remind the reader that a full NLO calculation would also require the higher order matching conditions for the SM and H^\pm contributions as well as the NLO anomalous dimensions for $C_7^{eff}(\mu)$. Nevertheless, we recall that preliminary results on the NLO corrections to $C_7^{eff}(\mu)$ indicate they are small[5], and a good approximation is obtained by employing the leading order expression for $C_7^{eff}(\mu)$ with the NLO matrix elements. Since this drastically reduces the μ dependence of the branching fraction, we would expect the H^\pm constraints to improve. Indeed, we find that the CLEO bound excludes the region to the left and beneath the curves in Fig. 12. For $m_t^{phys} = 169$ GeV we see that $m_{H^\pm} > 300$ GeV. This is calculated by using the same procedure that produced the previous charged Higgs mass bound by CLEO, *i.e.*, all the input parameters (*e.g.*, α_s , μ , m_c/m_b , and $B(B \rightarrow X\ell\nu)$) are varied over their allowed ranges in order to ascertain the most conservative limit. This bound holds in the general two-Higgs-doublet-model II, and in supersymmetry if the superpartners are all significantly massive.

4 Conclusion

In this paper we have studied the effects of supersymmetry to the FCNC observables concerning $b \rightarrow s$ transitions, and we have seen that deviations from the standard model could be detected with supersymmetric masses even at the TeV scale. This is especially true if $\tan\beta$ is very high. The large $\tan\beta$ enhancements in the $b \rightarrow s$ processes are unique. Deviations in $B - \bar{B}$ mixing are not as pronounced since the $m_b/\cos\beta$ enhancements, which are possible in this case, must be compared with m_t , whereas in the magnetic dipole $b \rightarrow s$ transitions the $m_b/\cos\beta$ enhancement is to be compared with m_b . Furthermore, the uncertainties in the decay constant and bag factor make $B - \bar{B}$ mixing observables slightly less appealing when trying to probe deviations from the standard model.

Therefore, it is possible that the first distinct signs of supersymmetry could come from deviations in $b \rightarrow s$ transitions. One would like direct confirmation of a possible deviation at the B -factory, and collider programs such as an upgraded luminosity Tevatron [41], and the LHC could provide it. At the Tevatron, the cleanest signal for supersymmetry is the $3l$ signal coming from leptonic decays of $p\bar{p} \rightarrow \chi_1^\pm \chi_2^0$. If the light charginos and neutralinos are mostly gaugino-like then the branching fraction into $3l$ can be quite high. This is true when the sleptons are lighter than the squarks and near M_W , as the slepton mediated decays of the gauginos enhance the final state leptons branching fraction. If the charginos and neutralinos contained a substantial Higgsino fraction then the slepton mediated exchanges are suppressed by lepton Yukawas to a negligible level, and all the decays must proceed through W and Z bosons, and recall that the branching fraction of $WZ \rightarrow l^+l^-l' \lesssim 2\%$ (not counting τ 's.) On the other hand, the $b \rightarrow s$ transitions are largest when there is a substantial Higgsino fraction in the lightest chargino state. The good news is that the tripleton signal and $b \rightarrow s$ decays are somewhat complementary in supersymmetric parameter space. The bad news is that confirmation between the two experiments might be difficult. Confirmation could be possible later at the LHC through total missing energy signatures, or at the NLC through direct mass and mixing angle measurements which would allow SUSY predicted $b \rightarrow s$ rates to be compared with the data.

Much of the signal phenomenology at high energy colliders such as the Tevatron and LHC rely on missing energy signatures. However, these are only possible with a stable LSP, which is the result of a postulated R-parity among the fields. R-parity conservation certainly need not hold in the correct theory of nature, and even tiny R-parity violating couplings destroy the missing energy signatures. More complicated analyses then must be performed with greatly reduced sensitivity to sparticle production. The Tevatron upgrade then would have difficulty exceeding equivalent

LEP II bounds on sparticle masses [42]. The LHC would have a significant search capability beyond LEP II, although much reduced compared to search capabilities with R-parity conservation if the LSP decays hadronically [43]. It appears to be difficult to extract SUSY signals at the LHC for superpartners above 1 TeV in this case. Searches for virtual sparticles, such as those we discuss in this paper, do not suffer in the presence of R-parity violation, and we have already noted that SUSY contributions are resolvable with masses above 1 TeV. In fact, the signal may be enhanced over the rate for gauge interactions alone if the R-parity violating couplings are sufficiently large. It is therefore possible that the B -factory could be sensitive to some parts in supersymmetric parameter space not accessible at the LHC.

Acknowledgements. We would like to thank C. Greub, Y. Grossman, A. Kagan, T. Rizzo, and M. Worah for helpful discussions.

Appendix

In this appendix all the standard model and supersymmetric contributions to the matching conditions $C_{7-10}(M_W)$ are listed in the limit that all squarks are degenerate except the stop squarks. It is also assumed that no sources of flavor violation are allowed other than the CKM angles.

The dipole moment operators $C_{7,8}(M_W)$ are already provided in the literature in several places for this limit. For completeness we write them down here using the formulas of [44] which are normalized according to our definition above:

$$\begin{aligned}
C_{7,8}^W(M_W) &= \frac{3}{2} x_W f_{\gamma,g}^{(1)}(x_W), \\
C_{7,8}^{H^\pm}(M_W) &= \frac{x_H}{2} \left[\frac{1}{\tan^2 \beta} f_{\gamma,g}^{(1)}(x_H) + f_{\gamma,g}^{(2)}(x_H) \right], \\
C_{7,8}^{\chi^\pm}(M_W) &= \sum_i \frac{M_W^2}{m_{\tilde{\chi}_i^\pm}^2} V_{i1}^2 f_{\gamma,g}^{(1)}(y_{\tilde{q}i}) - \sum_{i,k} \frac{M_W^2}{m_{\tilde{\chi}_i^\pm}^2} \Lambda_{ik}^2 f_{\gamma,g}^{(1)}(y_{ki}) \\
&\quad - \sum_i \frac{U_{i2}}{\sqrt{2} \cos \beta} \frac{M_W}{m_{\tilde{\chi}_i^\pm}} V_{i1} f_{\gamma,g}^{(3)}(y_{\tilde{q}i}) + \sum_{i,k} \frac{U_{i2}}{\sqrt{2} \cos \beta} \frac{M_W}{m_{\tilde{\chi}_i^\pm}} \Lambda_{ik} T_{k1} f_{\gamma,g}^{(3)}(y_{ki})
\end{aligned}$$

where

$$\begin{aligned}
x_W &= \frac{m_t^2}{M_W^2}, \quad x_H = \frac{m_t^2}{m_{H^\pm}^2}, \quad y_{\tilde{q}i} = \frac{m_{\tilde{q}}^2}{m_{\tilde{\chi}_i^\pm}^2}, \quad y_{ki} = \frac{m_{\tilde{t}_k}^2}{m_{\tilde{\chi}_i^\pm}^2}, \\
\Lambda_{ik} &= \frac{V_{i1} T_{k1} - V_{i2} T_{k2}}{\sqrt{2} M_W \sin \beta} m_t
\end{aligned}$$

and

$$\begin{aligned}
f_\gamma^{(1)}(x) &= \frac{7 - 5x - 8x^2}{36(x-1)^3} + \frac{x(3x-2)}{6(x-1)^4} \log x, \\
f_\gamma^{(2)}(x) &= \frac{3 - 5x}{6(x-1)^2} + \frac{3x-2}{3(x-1)^3} \log x, \\
f_\gamma^{(3)}(x) &= (1-x)f_\gamma^{(1)}(x) - \frac{x}{2}f_\gamma^{(2)}(x) - \frac{23}{36}, \\
f_g^{(1)}(x) &= \frac{2 + 5x - x^2}{12(x-1)^3} - \frac{x}{2(x-1)^4} \log x, \\
f_g^{(2)}(x) &= \frac{3-x}{2(x-1)^2} - \frac{1}{(x-1)^3} \log x, \\
f_g^{(3)}(x) &= (1-x)f_g^{(1)}(x) - \frac{x}{2}f_g^{(2)}(x) - \frac{1}{3}.
\end{aligned}$$

It is convenient to write $C_{9,10}(M_W)$ as

$$\begin{aligned}
C_9(M_W) &= \frac{Y - 4Z \sin^2 \theta_W}{\sin^2 \theta_W} \quad \text{and} \\
C_{10}(M_W) &= \frac{-Y}{\sin^2 \theta_W}.
\end{aligned}$$

The values for Y and Z are contained in [26] for arbitrary flavor structure and masses. For all squarks degenerate except the stop squarks and with only CKM flavor violation then

$$\begin{aligned}
Y &= Y_t + Y_{H^\pm}^Z + Y_{H^+}^\gamma + Y_{\chi^\pm}^Z + Y_{\chi^\pm}^\gamma + Y_{\chi^\pm}^{box}, \\
Z &= Z_t + Z_{H^\pm}^Z + Z_{H^+}^\gamma + Z_{\chi^\pm}^Z + Z_{\chi^\pm}^\gamma + Z_{\chi^\pm}^{box}.
\end{aligned}$$

The functional form of each of these contributions is

$$\begin{aligned}
Y_t &= \frac{4x_W - x_W^2}{8(1-x_W)} + \frac{3x_W^2}{8(1-x_W)^2} \log x_W, \\
Z_t &= \frac{108x_W - 259x_W^2 + 163x_W^3 - 18x_W^4}{144(1-x_W)^3} \\
&\quad + \frac{-8 + 50x_W - 63x_W^2 - 6x_W^3 + 24x_W^4}{72(1-x_W)^4} \log x_W, \\
Y_{H^+}^Z = Z_{H^+}^Z &= -\frac{1}{8} \cot^2 \beta x_W f_5(x_H), \\
Y_{H^+}^\gamma &= 0, \\
Z_{H^+}^\gamma &= -\frac{1}{72} \cot^2 \beta f_6(x_H), \\
Y_{\chi^\pm}^Z = Z_{\chi^\pm}^Z &= \sum_i -V_{i1}^2 L_1(m_{\tilde{\chi}_i^\pm}^2, m_{\tilde{q}}^2, m_{\tilde{q}}^2) + \sum_{i,k,l} \Lambda_{ki} \Lambda_{kl} T_{k1} T_{l1} L_1(m_{\tilde{\chi}_i^\pm}^2, m_{\tilde{t}_k}^2, m_{\tilde{t}_l}^2)
\end{aligned}$$

$$\begin{aligned}
& + \sum_{i,j} -V_{i1}V_{j1}L_2(m_{\tilde{q}}^2, m_{\tilde{\chi}_i^\pm}^2, m_{\tilde{\chi}_j^\pm}^2) + \sum_{i,j,k} \Lambda_{ki}\Lambda_{kj}L_2(m_{\tilde{t}_k}^2, m_{\tilde{\chi}_i^\pm}^2, m_{\tilde{\chi}_j^\pm}^2), \\
Y_{\chi^\pm}^\gamma & = 0, \\
Z_{\chi^\pm}^\gamma & = \sum_i -V_{i1}^2L_3(m_{\tilde{\chi}_i^\pm}^2, m_{\tilde{q}}^2) + \sum_{i,k} \Lambda_{ki}^2L_3(m_{\tilde{\chi}_i^\pm}^2, m_{\tilde{t}_k}^2), \\
Y_{\chi^\pm}^{box} & = \sum_{i,j} -V_{i1}V_{j1}L_4(m_{\tilde{\chi}_i^\pm}^2, m_{\tilde{\chi}_j^\pm}^2, m_{\tilde{q}}^2, m_{\tilde{\nu}}^2) + \sum_{i,j,k} \Lambda_{ki}\Lambda_{kj}L_4(m_{\tilde{\chi}_i^\pm}^2, m_{\tilde{\chi}_j^\pm}^2, m_{\tilde{t}_k}^2, m_{\tilde{\nu}}^2), \\
Z_{\chi^\pm}^{box} & = 0.
\end{aligned}$$

In the above equations $m_{\tilde{q}}$ is the common squark mass. The functions are defined as

$$\begin{aligned}
L_1(m_{\tilde{\chi}_i^\pm}^2, m_1^2, m_2^2) & = \frac{1}{2}c_2(m_{\tilde{\chi}_i^\pm}^2, m_1^2, m_2^2) \\
L_2(m^2, m_{\tilde{\chi}_i^\pm}^2, m_{\tilde{\chi}_j^\pm}^2) & = -\frac{1}{2}c_2(m^2, m_{\tilde{\chi}_i^\pm}^2, m_{\tilde{\chi}_j^\pm}^2)V_{i1}V_{j1} \\
& \quad + \frac{1}{4}m_{\tilde{\chi}_i^\pm}m_{\tilde{\chi}_j^\pm}c_0(m^2, m_{\tilde{\chi}_i^\pm}^2, m_{\tilde{\chi}_j^\pm}^2)U_{i1}U_{j1}, \\
L_3(m_{\tilde{\chi}_i^\pm}^2, m^2) & = \frac{M_W^2}{36m^2}f_7(m_{\tilde{\chi}_i^\pm}^2/m^2), \\
L_4(m_{\tilde{\chi}_i^\pm}^2, m_{\tilde{\chi}_j^\pm}^2, m_{\tilde{q}}^2, m_{\tilde{\nu}}^2) & = M_W^2d_2(m_{\tilde{\chi}_i^\pm}^2, m_{\tilde{\chi}_j^\pm}^2, m_{\tilde{q}}^2, m_{\tilde{\nu}}^2)V_{i1}V_{j1}.
\end{aligned}$$

These L -functions are expressed in terms of functions contained in [26] and are explicitly given by

$$\begin{aligned}
f_5(x) & = \frac{x}{1-x} + \frac{x}{(1-x)^2} \log x, \\
f_6(x) & = \frac{38x - 79x^2 + 47x^3}{6(1-x)^3} + \frac{4x - 6x^2 + 3x^4}{(1-x)^4} \log x, \\
f_7(x) & = \frac{52 - 101x + 43x^2}{6(1-x)^3} + \frac{6 - 9x + 2x^3}{(1-x)^4} \log x, \\
c_0(m_1^2, m_2^2, m_3^2) & = -\left[\frac{m_1^2 \log \frac{m_1^2}{\mu^2}}{(m_1^2 - m_2^2)(m_1^2 - m_3^2)} + (m_1 \leftrightarrow m_2) + (m_1 \leftrightarrow m_3) \right], \\
c_2(m_1^2, m_2^2, m_3^2) & = \frac{3}{8} - \frac{1}{4} \left[\frac{m_1^4 \log \frac{m_1^2}{\mu^2}}{(m_1^2 - m_2^2)(m_1^2 - m_3^2)} + (m_1 \leftrightarrow m_2) + (m_1 \leftrightarrow m_3) \right], \\
d_2(m_1^2, m_2^2, m_3^2, m_4^2) & = -\frac{1}{4} \left[\frac{m_1^4 \log \frac{m_1^2}{\mu^2}}{(m_1^2 - m_2^2)(m_1^2 - m_3^2)(m_1^2 - m_4^2)} \right. \\
& \quad \left. + (m_1 \leftrightarrow m_2) + (m_1 \leftrightarrow m_3) + (m_1 \leftrightarrow m_4) \right].
\end{aligned}$$

References

- [1] A. Buras, Plenary talk given at the *28th International Conference on High Energy Physics*, Warsaw, Poland, July 1996.
- [2] A. Buras, M. Misiak, M. Münz, S. Pokorski, Nucl. Phys. B **424** (1994) 374.
- [3] C. Greub, T. Hurth, and D. Wyler, Phys. Lett. B **380** (1996) 385; Phys. Rev. D **54** (1996) 3350; C. Greub and T. Hurth, talk presented at DPF96, Minneapolis, MN, August 1996, hep-ph/9608449.
- [4] A.J. Buras and M. Münz, Phys. Rev. D **52** (1995) 186.
- [5] K.G. Chetyrkin, M. Misiak, and M. Münz, in preparation; M. Misiak, talk presented at ICHEP96, Warsaw, Poland, July 1996.
- [6] CLEO Collaboration, M.S. Alam *et al.*, Phys. Rev. Lett. **74** (1995) 2885.
- [7] CLEO Collaboration, R. Balest *et al.*, in *Proceedings of the 27th International Conference on High Energy Physics*, Glasgow, Scotland, 1994, edited by P.J. Bussey and I.G. Knowles (IOP, London, 1995); CDF Collaboration, C. Anway-Wiese, in *The Albuquerque Meeting*, Proceedings of the 8th Meeting of the Division of Particles and Fields of the American Physical Society, Albuquerque, New Mexico, 1994, edited by S. Seidel (World Scientific, Singapore, 1995).
- [8] A. Ali, T. Mannel, and T. Morozumi, Phys. Lett. B **273** (1991) 505.
- [9] A. Ali, G.F. Giudice, and T. Mannel, Zeit. für Physik C **67** (1995) 417.
- [10] J.L. Hewett, Phys. Rev. D **53** (1996) 4964.
- [11] See, for example, B. Grinstein, M.J. Savage, and M. Wise, Nucl. Phys. B **319** (1989) 271; A. Ali, in *20th International Nathiagali Summer College on Physics and Contemporary Needs*, Bhurban, Pakistan, 1995, hep-ph/9606324.
- [12] T. Inami and C.S. Lim, Prog. Theor. Phys. **65**, 297 (1981).
- [13] R.M. Barnett, *et al.*, (Particle Data Group), Phys. Rev. D **54** (1996) 1.
- [14] M. Schmelling, Plenary talk given at the *28th International Conference on High Energy Physics*, Warsaw, Poland, July 1996.
- [15] P. Tipton, talk presented at *28th International Conference on High Energy Physics*, Warsaw, Poland, July 1996.

- [16] J. Richman, Plenary talk given at the *28th International Conference on High Energy Physics*, Warsaw, Poland, July 1996.
- [17] N.G. Deshpande, J. Trampetic, and K. Panrose, *Phys. Rev. D* **39** (1989) 1461; C.S. Lim, T. Morozumi, and A.I. Sanda, *Phys. Lett. B* **218** (1989) 343; Z. Ligeti and M. Wise, *Phys. Rev. D* **53** (1996) 4937.
- [18] A. Ali and C. Greub, *Zeit. für Physik C* **49** (1991) 431; *Phys. Lett. B* **259** (1991) 182; *Phys. Lett. B* **361** (1995) 146; N. Pott, *Phys. Rev. D* **54** (1996) 938.
- [19] K. Adel and Y.-P. Yao, *Phys. Rev. D* **49** (1994) 4945.
- [20] J. Chay, H. Georgi, and B. Grinstein, *Phys. Lett. B* **247** (1990) 399; I. Bigi, N. Uraltsev, and A. Vainshtein, *Phys. Lett. B* **243** (1992) 430; B. Blok and M. Shifman, *Nucl. Phys. B* **399** (1993) 441; I. Bigi *et al.*, *Phys. Rev. Lett.* **71** (1993) 496.
- [21] Y. Nir, N. Seiberg, *Phys. Lett. B* **309** (1993) 337.
- [22] M. Dine, A. Nelson, *Phys. Rev. D* **48** (1993) 1277; M. Dine, A. Nelson, Y. Shirman, *Phys. Rev. D* **51** (1995) 1362.
- [23] S. Dimopoulos, S. Thomas, J.D. Wells, hep-ph/9609434.
- [24] S. Dimopoulos, H. Georgi, *Nucl. Phys. B* **193** (1981) 150.
- [25] S. Bertolini, F. Borzumati, A. Masiero, G. Ridolfi, *Nucl. Phys. B* **353** (1991) 591. F. Borzumati, *Zeit. für Physik C* **63** (1994) 291; F. Gabbiani, E. Gabrielli, A. Masiero, L. Silvestrini, hep-ph/9604387; V. Barger, M.S. Berger, P. Ohmann, R.J.N. Phillips, *Phys. Rev. D* **51** (1995) 2438; D. Choudhury, F. Eberlein, A. König, J. Louis, S. Pokorski, *Phys. Lett. B* **342** (1995) 180; J. Lopez, D. Nanopoulos, X. Wang, A. Zichichi, *Phys. Rev. D* **51** (1995) 147.
- [26] P. Cho, M. Misiak, D. Wyler, hep-ph/9601360.
- [27] For description of procedure we follow, see G.L. Kane, C. Kolda, L. Roszkowski, J. Wells, *Phys. Rev. D* **49** (1994) 6173.
- [28] We are neglecting potentially important contributions coming from disparate SUSY and electroweak scales, for a discussion of this see H. Anlauf, *Nucl. Phys. B* **430** (1994) 245.
- [29] L. Randall, R. Sundrum, *Phys. Lett. B* **312** (1993) 148; B. Grinstein, Y. Nir, and J.M. Soares, *Phys. Rev. D* **48** (1993) 3960; A. Nelson, M. Strassler, hep-ph/9607362.

- [30] M. Boulware, D. Finnell, Phys. Rev. D **44** (1991) 2054; J.D. Wells, C. Kolda, G.L. Kane, Phys. Lett. B **338** (1994) 219.
- [31] M. Carena, M. Quiros, C. Wagner, Phys. Lett. B **380** (1996) 81.
- [32] H. Haber, G.L. Kane, Phys. Rep. 142B (1984) 212.
- [33] A. Brignole, F. Feruglio, F. Zwirner, hep-ph/9601293.
- [34] R. Garisto, J. Ng, Phys. Lett. B **315** (1993) 372.
- [35] L. Hall, R. Rattazzi, U. Sarid, Phys. Rev. D **50** (1994) 7048.
- [36] D. Pierce, J. Bagger, K. Matchev, R. Zhang, hep-ph/9606211.
- [37] Y. Okada, Phys. Lett. B **315** (1993) 119.
- [38] J.L. Hewett, Phys. Rev. Lett. **70** (1993) 1045, V. Barger, M. Berger, and R.J.N. Phillips, Phys. Rev. Lett. **70** (1993) 1368; V. Barger, J. Hewett, R. Phillips, Phys. Rev. D **41** (1990) 3421; N. Deshpande, K. Panose, J. Trampetic, Phys. Lett. B **308** (1993) 322.
- [39] T.G. Rizzo, Phys. Rev. D **38** (1988) 820; X.G. He *et al.*, Phys. Rev. D **38** (1988) 814; W.S. Hou and R.S. Willey, Phys. Lett. B **202** (1988) 591; C.Q. Geng and J.N. Ng, Phys. Rev. D **38** (1988) 2858; B. Grinstein, R. Springer, and M. Wise, Nucl. Phys. B **339** (1990) 269.
- [40] P. Krawczyk and S. Pokorski, Phys. Rev. Lett. **60** (1988) 182; Y. Grossman, H. Haber, and Y. Nir, Phys. Lett. B **357** (1995) 630.
- [41] H. Baer, C.-h. Chen, C. Kao, X. Tata, Phys. Rev. D **52** (1995) 1565; S. Mrenna, G.L. Kane, G. Kribs, J.D. Wells, Phys. Rev. D **53** (1996) 1168.
- [42] D.P. Roy, Phys. Lett. B **283** (1992) 270; H. Baer, C. Kao, X. Tata, Phys. Rev. D **51** (1995) 2180.
- [43] H. Baer, C.-h. Chen, X. Tata, hep-ph/9608221.
- [44] R. Barbieri, G. Giudice, Phys. Lett. B **309** (1993) 86.